Acta Cryst. (1983). A**39**, 38–46

The Resolution Function of a Perfect-Crystal Three-Axis X-ray Spectrometer

BY R. PYNN

Institut Laue–Langevin, 156X, 38042 Grenoble CEDEX, France

AND Y. FUJII AND G. SHIRANE

Brookhaven National Laboratory, Upton, NY 11973, USA

(*Received* 3 *March* 1982; *accepted* 20 *July* 1982)

Abstract

The resolution function of a three-axis, X-ray spectrometer is considered for the case when the monochromator and analyser crystals are ideally perfect. It is shown that, for X-ray sources which produce either an ill-collimated monochromatic beam (conventional source) or a well-collimated white beam (synchrotron radiation), the resolution problem may be simplified. This simplification allows the profile of an arbitrary section of the resolution function to be expressed as a one-dimensional integral of the product of three functions; one to represent the source characteristics and the other two to describe the Darwin profiles of the monochromator and analyser crystals. The formalism is extended to describe the measurement of the resolution function by a perfect crystal mounted on the sample table of the spectrometer. Comparison of the *a priori* calculations with measurements made on a spectrometer at a conventional source yields very good agreement.

Introduction

Recently intense X-ray sources such as high-brilliance rotating-anode generators and synchrotron radiation sources have enabled high-resolution diffraction experiments to explore new areas in science. In condensed-matter physics, for example, particular interest has been focused on phase transitions in low-dimensional systems such as smectic liquid crystals (see, for example, Als-Nielsen *et al.*, 1980) and on the physics of physisorbed systems (Birgeneau, Brown, Horn, Moncton & Stephens, 1981; Nielsen, Als-Nielsen, Bohr & McTague, 1981; Sinha, 1980). The X-ray diffraction technique affords great advantages in such studies because it yields direct information about the spatial correlations of constituent atoms. The high momentum resolution ($\Delta Q \lesssim 10^{-4}$ Å^{-1}) required for the precise measurement of diffraction profiles is generally achieved by using a three-axis spectrometer with perfect crystals as monochromator and analyser. Such a configuration reduces the resolution volume in the reciprocal space of the sample by a factor of between 10 and 100 compared with that obtainable with a conventional diffractometer equipped with mosaic crystals. However, even when perfect crystals are used, the correction for instrumental resolution is sometimes crucial to obtaining an adequate correlation function from the observed spectra.

The calculation of resolution properties must account correctly for the dynamical diffraction of X-rays by the perfect monochromator and analyser crystals. Although the theory of dynamical diffraction is well known (Zachariasen, 1945; Batterman & Cole, 1964), it is usually applied to calculations of the rocking curves of perfect crystals (Kikuta & Kohra, 1970; Kikuta, 1970) rather than to the convolution of effects which contribute to the resolution function of a three-axis spectrometer.

In contrast to the X-ray case, several methods have been developed for the calculation of the resolution properties of *neutron* three-axis spectrometers (Stedman, 1968; Cooper & Nathans, 1967). These methods are, however, not directly applicable to the perfect-crystal X-ray spectrometer because they assume that mosaic crystals are used as optical elements and that kinematical scattering theory can therefore be applied. The latter theory is inadequate for the perfect-crystal spectrometer for two fundamental reasons. Firstly, it accounts only for the misorientation of diffracting atomic planes (mosaic spread) and ignores the effective uncertainty in interplanar spacing which is the dominant effect in diffraction by perfect crystals. Secondly, the distribution of mosaic grains, which is reproduced as the rocking curve of a crystal, is approximately Gaussian. This is not the case for a perfect crystal whose rocking curve has the characteristic long-tailed, asymmetric form of the Darwin profile.

In the present paper we calculate the resolution function for a perfect-crystal three-axis spectrometer installed either at a conventional source or at a

0567-7394/83/010038-09$01.50

synchrotron radiation facility. Our method is based on that developed by Bjerrum-Möller & Nielsen (1969*a*,*b*) for the equivalent neutron spectrometer but accounts fully for all effects of dynamical diffraction. The calculations are compared with measurements made with a conventional source in several different spectrometer configurations.

Bragg diffraction by a perfect crystal

The monochromator and analyser crystals of the spectrometers considered in this paper are assumed to be perfect crystals. Bragg diffraction is thus described by the dynamical scattering theory as propounded, for example, by Zachariasen (1945). Since this theory is essential to the present calculation, its salient elements are recalled in this section.

Consider a ray of wavevector $\mathbf{k}_1$ incident on a crystal surface and diffracted as a ray of wavevector $\mathbf{k}_2$. As indicated in Fig. 1 the crystal surface is not necessarily parallel to the diffracting planes; rather there is an angle φ between the surface and the planes. It is convenient to specify the asymmetry of the surface cut by a parameter b, related to φ according to

$$b = \frac{\sin(\varphi - \theta_B)}{\sin(\varphi + \theta_B)} \leq 0, \tag{1}$$

where θ_B is the usual kinematical Bragg angle defined by

$$\lambda = 2d \sin \theta_B. \tag{2}$$

Here d is the spacing of the diffracting planes (see Fig. 1) and λ is the wavelength of the scattered radiation. The introduction of the parameter b allows the relationship between the angle of incidence (θ_1) and the angle of diffraction (θ_2) to be written in a simple form, *viz*

$$\theta_2 = \theta_B - b(\theta_1 - \theta_B). \tag{3}$$

Equation (3) demonstrates, for example, that if a narrow monochromatic but divergent beam is incident on a crystal surface for which $|b|$ is small (*i.e.* $\theta_B \sim \varphi$) a wide beam with a smaller divergence is produced after diffraction.

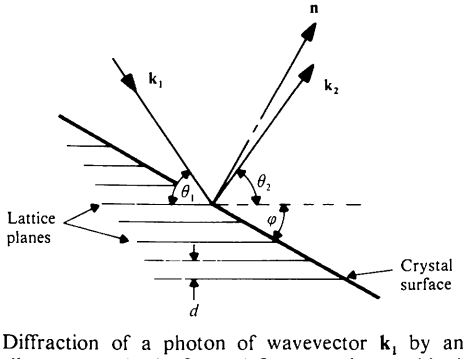

Fig. 1. Diffraction of a photon of wavevector $\mathbf{k}_1$ by an asymmetrically cut crystal. The figure defines notation used in the text.

The dynamical theory of Bragg diffraction from a crystal is couched in terms of two parameters denoted by y and g and defined according to

$$g = -\frac{(1-b)\mu_0\lambda}{4\pi K|\Psi'_H||b|^{1/2}} \tag{4}$$

$$y = \frac{(1-b)(n-1) + b\chi/2}{K|\Psi'_H||b|^{1/2}}. \tag{5}$$

In these equations μ_0 is the absorption coefficient of the crystal and n its index of refraction. Thus g is related to the dissipative part of the scattering while y is described in terms of the real parts of the atomic scattering amplitudes. In (4) and (5)

$$\chi = 4 \sin \theta_B \{\sin \theta_B - \sin \theta_1\}, \tag{6}$$

$K = 1$ if the radiation is polarized perpendicular to the scattering plane and $K = |\cos 2\theta_B|$ if the polarization direction is parallel to this plane. The remaining quantity in (4), (5), *viz* Ψ'_H, is defined in terms of the structure factor F_H for the scattering planes. Thus

$$\Psi_H = -\frac{1}{\pi}\left(\frac{e^2}{mc^2}\right)\frac{\lambda^2}{v_a}F_H \equiv \Psi'_H + i\Psi''_H \tag{7}$$

with e^2/mc^2 as the classical electron radius and v_a as the volume of the crystal unit cell. The real and imaginary parts of the structure factor F_H are defined as usual by

$$F'_H = \sum_j (f_j^0 + \Delta f'_j)\exp(i\boldsymbol{\tau}_H.\mathbf{r}_j)\exp(-W_j) \tag{8a}$$

and

$$F''_H = \sum_j \Delta f''_j \exp(i\boldsymbol{\tau}_H.\mathbf{r}_j)\exp(-W_j), \tag{8b}$$

where f_j^0, $\Delta f'_j$ and $\Delta f''_j$ are the mean atomic scattering factor and the real and imaginary dispersion corrections for an atom situated at position $\mathbf{r}_j$ in the unit cell, $\boldsymbol{\tau}_H$ is the reciprocal-lattice vector for the diffraction planes and W_j is the Debye–Waller factor for the atom j.

In terms of the parameters defined above the diffracted intensity I_2 is related to the incident intensity I_1 by

$$\frac{I_2}{I_1} = |b|\{L - [L^2 - (1 + 4\kappa^2)^2]^{1/2}\}, \tag{9}$$

where

$$\kappa = \Psi''_H/\Psi'_H \tag{10}$$

and

$$L = |\{(-1 + y^2 - g^2)^2 + 4(gy - \kappa)^2\}^{1/2}| + y^2 + g^2. \tag{11}$$

In the case of a non-absorbing crystal κ and g are zero and (9) reduces to the familiar Darwin (1914) result. Since the incident and diffracted beams have different widths for $\varphi \neq 0$, the incident and diffracted powers are related by

$$\frac{P_2}{P_1} = \frac{1}{|b|}\frac{I_2}{I_1}. \tag{12}$$

For the resolution calculation presented here the interesting quantity is the beam power per unit area, given by I_1 or I_2.

The reflection profile described by (9) is fundamentally different from that obtained from the kinematical theory of diffraction by a mosaic crystal. In the latter case the scattering angle for any ray of wavelength λ is assumed to be $2\theta_B$ so that

$$\theta_1^{\text{kinematic}} + \theta_2^{\text{kinematic}} = 2\theta_B. \tag{13}$$

Thus if $\theta_1^{\text{kinematic}}$ *in*creases, $\theta_2^{\text{kinematic}}$ *de*creases. In the dynamical theory of scattering by a symmetrically cut crystal ($b = -1$), θ_1 and θ_2 are *equal* [*cf.* (3)] and, for a particular λ, a band of values of θ_2 distributed according to the Darwin profile is diffracted. It is as if the X-rays were diffracted according to a Bragg law by a crystal in which the *length* of the reciprocal-lattice vector $\boldsymbol{\tau}_H$ was uncertain and distributed according to the Darwin function. In a mosaic crystal this effect is completely dominated by the distribution of *orientations* of $\boldsymbol{\tau}_H$ which represents the mosaic spread.

General formulation of the resolution problem

In a scattering experiment the measured intensity I depends both on the scattering properties of the sample and the transmission function of the instrument. Quite generally we may write

$$I \propto \int \mathrm{d}\mathbf{k}_i \int \mathrm{d}\mathbf{k}_f P_i(\mathbf{k}_i)\, S(\mathbf{k}_i \rightarrow \mathbf{k}_f)\, P_f(\mathbf{k}_f), \tag{14}$$

where $P_i(\mathbf{k}_i)$ is the probability that a photon of wavevector $\mathbf{k}_i$ is incident on the sample, $P_f(\mathbf{k}_f)$ the probability that a photon of wavevector $\mathbf{k}_f$ is transmitted by the analyser system and $S(\mathbf{k}_i \rightarrow \mathbf{k}_f)$ the probability that the sample scatters a photon from $\mathbf{k}_i$ to $\mathbf{k}_f$. The finite resolution of the instrument arises because the probabilities P_i and P_f are non-zero for wavevectors other than the mean initial and final wavevectors, denoted $\mathbf{k}_I$ and $\mathbf{k}_F$. Both P_i and P_f involve contributions from the Darwin widths of the monochromator and analyser crystals discussed in the previous section. In addition, there is a contribution to P_i which depends on the X-ray source characteristics.

The fluctuation spectrum of the sample $S(\mathbf{k}_i \rightarrow \mathbf{k}_f)$ does not depend on $\mathbf{k}_i$ and $\mathbf{k}_f$ separately but rather on the scattering vector $\mathbf{Q}$ and energy transfer $\hbar\omega$ defined by the conservation equations

$$\mathbf{Q} = \mathbf{k}_i - \mathbf{k}_f \tag{15a}$$

$$\omega = c(|k_i| - |k_f|), \tag{15b}$$

where c is the velocity of light *in vacuo*. In terms of these variables (14) becomes

$$I(\mathbf{Q}_0,\omega_0) \sim \int\int\int \mathrm{d}^3 Q \int \mathrm{d}\omega S(\mathbf{Q},\omega)\, R(\mathbf{Q} - \mathbf{Q}_0, \omega - \omega_0), \tag{16}$$

where $\mathbf{Q}_0$ and ω_0 are obtained from (15) with the mean initial and final wavevectors $\mathbf{k}_I$ and $\mathbf{k}_F$. The function R in (16) is the instrumental resolution defined by integrating the product $P_i P_f$ over $\mathbf{k}_i$ and $\mathbf{k}_f$ subject to the constraint imposed by (15). Since the component of $\mathbf{Q}$ perpendicular to the scattering plane (defined by $\mathbf{k}_I$ and $\mathbf{k}_F$) is not correlated with the other components of $\mathbf{Q}$ or with ω, the integration over this component, denoted Q_z, can be carried out independently. For the moment we consider only the resolution function in the remaining three dimensions, namely ω and the components of $\mathbf{Q}$ in the scattering plane.

The independent-distribution method

The difference between $\mathbf{k}_i$ and $\mathbf{k}_I$ (in the scattering plane) may be written in component form as (*cf.* Fig. 2)

$$\Delta_i^{\parallel} = (k_i - k_I)/k_I \tag{17a}$$

$$\Delta_i^{\perp} = \theta_i - \theta_I, \tag{17b}$$

where θ_i is the angle of incidence on the sample and θ_I is the mean value of this quantity. In general P_i is a non-separable function of $\Delta_i^{\parallel}$ and $\Delta_i^{\perp}$. However, it may be possible to find a transformation to two new variables $\mathbf{x}_1$ and $\mathbf{x}_2$, as shown in the second part of Fig. 2, which allows P_i to be written as the product of a function of $\mathbf{x}_1$ only and another function of $\mathbf{x}_2$ only. This procedure was first used for the calculation of the resolution properties of a *neutron* three-axis spectrometer by Stedman (1968) and was subsequently investigated in more detail by Bjerrum-Móller & Nielsen (1969*a*,*b*). The method has the advantage that each probability function may be convolved independently with the sample fluctuation spectrum $S(\mathbf{Q},\omega)$. In the case where the probability functions may be approximated by Gaussian curves (the neutron spectrometer for example) an even greater simplification is afforded. The width of a scan through a (planar) phonon dispersion surface or through a Bragg point is given, in this instance, by a simple quadrature addition of the widths of the individual probability functions. Different contributions to the instrumental resolution, arising from the different $\mathbf{x}_j$ are therefore decoupled. For a neutron three-axis spectrometer, for example, mono-

chromator and analyser contributions to the scan width may be separated and each may be varied independently to achieve an optimum experimental configuration.

Even in cases where the probability functions P_i and P_f are non-Gaussian the formalism described above may be useful. Provided the second moment of the P's is defined, the central limit theorem indicates that characteristic widths of the probability functions can be treated in the same way as Gaussian widths to give an estimate of a scan width which is useful in the optimization of spectrometer design.

Resolution function for a perfect-crystal spectrometer

The technique outlined above can be applied to a perfect-crystal X-ray spectrometer placed either on a conventional source or installed at a synchrotron radiation facility. Since the resolution calculation is not identical for the two sources we choose to sacrifice generality for simplicity of presentation and give in detail only the calculation for a conventional source such as a rotating-anode generator.

Consider first a perfect-crystal monochromator represented by Fig. 1. Define $P_1(\theta_1,k)$ as the probability that a photon of wavevector $\mathbf{k}$ is incident at an angle θ_1 and $P(\theta_2,k)$ as the probability of observing a diffracted photon defined by (θ_2,k). Then

$$P_2(\theta_2,k) = P_1(\theta_1,k)\, D_M(y_{12}), \tag{18}$$

where y_{12} is obtained from (5) and D_M is the monochromator Darwin function given by (9). Although D_M is a function of both g and y the variation of the former quantity is negligible for the range of wavevectors reflected and a suitable mean value may be chosen. Since the X-ray source is a characteristic spectral line, $P_1(\theta_1,k)$ is a sharply peaked function of $\mathbf{k}$ but is essentially independent of θ_1. Thus it is reasonable to write

$$P_1(\theta_1,k) = \frac{(k_0\sigma_k)^2}{(k-k_0)^2 + \sigma_k^2 k_0^2} = \frac{\sigma_k^2}{(\Delta^{\parallel})^2 + \sigma_k^2}, \tag{19}$$

where k_0 is the mean wavevector of the characteristic X-ray line of half-width σ_k and $\Delta^{\parallel}$ is defined by (17) with k and k_0 substituted for k_i and k_f respectively.

The monochromator orientation is adjusted so that for the mean angle of incidence, θ_{10}, one obtains $y = 0$ for the wavevector k_0. Thus

$$y_{12} = \alpha\Delta_2^{\parallel} + \beta\Delta_2^{\perp}, \tag{20}$$

where $\Delta_2^{\perp} = \theta_2 - \theta_{20}$ and α and β are the derivatives of y with respect to k and θ_2. Straightforward differentiation yields

$$\alpha \equiv k\frac{\partial y}{\partial k} \simeq -\frac{2b\sin^2\theta_B}{|b|^{1/2}K|\Psi_H'|} \tag{21a}$$

$$\beta \equiv \frac{\partial y}{\partial \theta_2} \simeq \frac{\sin 2\theta_B}{|b|^{1/2}K|\Psi_H'|}. \tag{21b}$$

To apply the independent distribution method it is necessary to transform $\Delta^{\parallel}$ and $\Delta^{\perp}$ to new variables $\mathbf{x}_1$ and $\mathbf{x}_2$ according to (*cf.* Fig. 2)

$$x_1\cos u_1 + x_2\cos u_2 = k_0\Delta_2^{\parallel} \tag{22a}$$

$$x_1\sin u_1 + x_2\sin u_2 = k_0\Delta_2^{\perp}. \tag{22b}$$

Since P_1 [(19)] depends only on $\Delta^{\parallel}$ the choice

$$u_1 = \pi/2; \quad \tan(\varepsilon_M\varepsilon_S u_2) = \alpha_M/\beta_M \tag{23}$$

implies that P_1 is a function of x_2 only and that D_M is a function of x_1 only. A calculation similar to the above for the analyser crystal yields (see Fig. 2 for definitions)

$$u_3 = \pi/2; \quad \tan(\varepsilon_S\varepsilon_A u_4) = -\alpha_A/b\beta_A. \tag{24}$$

In (23) and (24) the quantities ε_M, ε_S and ε_A account for the different possible scattering senses at the monochromator, sample and analyser respectively. $\varepsilon = +1$ for scattering to the right and $\varepsilon = -1$ for scattering to the left. The scattering triangle drawn in Fig. 2 corresponds to $\varepsilon_M = \varepsilon_A = -1$ and $\varepsilon_S = 1$. The latter figure also defines the senses in which the angles u_j are to be construed as positive.

Fig. 3 is an attempt to summarize pictorially the results obtained above in a three-dimensional representation of real and reciprocal space. An uncollimated beam with a Lorentz wavelength distribution is incident on a symmetrically cut perfect crystal. In the scattered

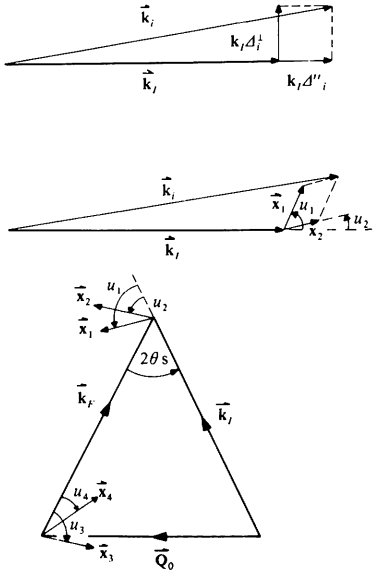

Fig. 2. The upper two parts of the figure demonstrate the change of variable from Δ to $\mathbf{x}$ as specified in (22). The lower figure is the scattering triangle used in this paper and serves to define the senses in which the angles u_j are positive.

beam the Lorentzian spread is reproduced along $\mathbf{x}_2$. Since, from (21), $\alpha/\beta = \tan\theta_B$, (24) yields $u_2 = -\theta_B$. Thus $\mathbf{x}_2$ is parallel to the diffracting planes of the crystal. The Darwin profile of the crystal is reproduced in the diffracted beam along $\mathbf{x}_1$ which is perpendicular to the propagation direction of this beam. A heuristic argument which explains these results is not difficult to find. If the incident beam is perfectly monochromatic but uncollimated the distribution of wavevectors in the diffracted beam must be perpendicular to the latter because $\theta_1 = \theta_2$ are the only variables in the problem. Further, for any given incident wavevector the most probable diffracted ray corresponds to $y = 0$ and hence, from (6), to $\theta_1 \simeq \theta_B$. Thus, Bragg's law $\tau_H = 2k_2 \sin\theta_2$ may be used to relate k_2 and θ_2. Differentiation of this leads immediately to $\Delta_2^{\perp}/\Delta_2^{\parallel} = -\tan\theta_B$ and thus to the fact that the distribution of incident wavevectors is reproduced along a direction parallel to the reflecting planes.

In summary, the probability that a photon with an incident wavevector

$$\mathbf{k}_i = \mathbf{k}_I + \mathbf{x}_1 + \mathbf{x}_2$$

and a final wavevector

$$\mathbf{k}_f = \mathbf{k}_F + \mathbf{x}_3 + \mathbf{x}_4$$

is transmitted by the spectrometer is given by

$$T = P_M(x_2/X_2)\, D_M(x_1/X_1)\, P_A(x_4/X_4)\, D_A(x_3/X_3), \quad (25)$$

where X_j are scale lengths for the various distributions; they are the half-widths for the Lorentzian functions P_M and P_A and the values of x_1 and x_3 which yield $y = 1$ for the monochromator and analyser Darwin functions. Thus we have

$$X_1 = k/\beta_M \quad (26a)$$

$$X_2 = \sigma_k k/\cos u_2 \quad (26b)$$

$$X_3 = -k/b_A\beta_A \quad (26c)$$

$$X_4 = \infty, \quad (26d)$$

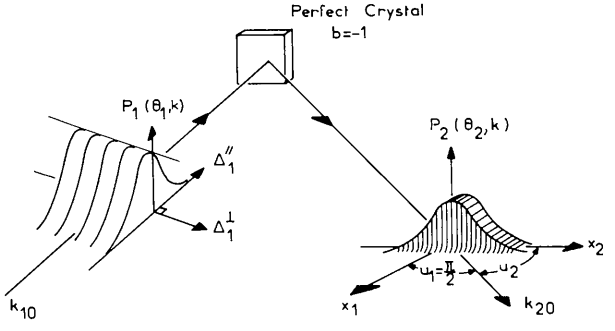

Fig. 3. An attempt to portray the scattering of an uncollimated 'monochromatic' X-ray beam by a perfect crystal. The wavelength distribution of the incident beam is reproduced along $\mathbf{x}_2$ while the Darwin profile of the reflecting crystal appears along $\mathbf{x}_1$.

where $|\mathbf{k}_I| = |\mathbf{k}_F| = k$ and subscripts M and A correspond respectively to the monochromator and analyser crystals. X_4 is infinite because the detector does not distinguish between photons of different wavelengths.

Width of a scan

In this section we calculate the intensity distribution obtained when a Bragg reflection from a sample crystal is scanned. To generate this resolution profile we assume that the Bragg reflection corresponds to a Dirac δ function located at wavevector $\boldsymbol{\tau}$. The intensity recorded when the spectrometer is set to measure at $\mathbf{Q} = \boldsymbol{\tau} + \delta\mathbf{Q}$ is

$$R(\delta\mathbf{Q}) = \int\int\int\int \mathrm{d}^4(x_i)\, P_M(x_2/X_2)\, D_M(x_1/X_1)\, P_A(x_4/X_4) \times D_A(x_3/X_3)\, \delta(\boldsymbol{\tau} - \mathbf{Q} - \mathbf{x}_1 - \mathbf{x}_2 + \mathbf{x}_3 + \mathbf{x}_4) \times \delta(\mathbf{x}_2\cos u_2 - \mathbf{x}_4\cos u_4). \quad (27)$$

The final δ function in this expression is included because the (Bragg) scattering from the sample is assumed to be elastic.

Since $X_4 = \infty$ the integration of (27) over x_4 may be carried out trivially to remove one of the δ functions. The remaining δ function yields two constraints involving x_1, x_2 and x_3. Solving for x_1 and x_3 in terms of x_2 (say) allows (27) to be written, after some simple manipulation, as

$$R(\delta\mathbf{Q}) = \int \mathrm{d}x_2\, P_M(x_2/X_2)\, D_M[(B_0 + B_2 x_2)/X_1] \times D_A[(A_0 + A_1 B_0 + \{A_1 B_2 + A_2\}\, x_2)/X_3], \quad (28)$$

where

$$B_0 = \frac{\delta Q_{\parallel}\sin\theta_s - \delta Q_{\perp}\cos\theta_s}{2\sin\theta_s\cos\theta_s}$$

$$B_2 = \frac{-\sin(\theta_s + u_2)}{\cos\theta_s}$$

$$A_0 = \frac{\delta Q_{\parallel}}{\cos\theta_s}; \quad A_1 = -1 \quad (29)$$

$$A_2 = -[\cos u_4\, \sin(\theta_s + u_2) + \cos u_2 \times \sin(\theta_s + u_4)]/[\cos u_4\cos\theta_s].$$

Here $\delta Q_{\parallel}$ and $\delta Q_{\perp}$ are the components of $\delta\mathbf{Q}$ parallel and perpendicular to $\mathbf{Q}$ and $2\theta_s$ in the mean scattering angle at the sample (*cf.* Fig. 2).

Equation (28) is a one-dimensional integral which may be evaluated simply by numerical means. Several such calculations will be compared with experiment below.

Gaussian approximation

In many cases an *approximate* scan width may be calculated without recourse to numerical integration. Since (28) involves the convolution of three functions we may hope that, to a reasonable approximation, each function can be replaced by a Gaussian of the appropriate second moment. This is a heuristic application of the central limit theorem. Unfortunately, in a strict sense, the second moment of the Darwin function is undefined. However, we have found that a reasonable approximation is to treat X_1 and X_3 as if they were standard deviations. Then the width of the scan is given by

$$\sigma^2 = \frac{X_1^2 X_3^2 + B_2^2 X_2^2 X_3^2 + (A_2 + A_1 B_2)^2 X_1^2 X_2^2}{B_0^2 X_3^2 + (A_0 + A_1 B_0)^2 X_1^2 + (B_0 A_2 - A_0 B_2)^2 X_2^2}. \quad (30)$$

The treatment of X_j as the standard deviations of various resolution distributions mimics exactly the calculation of Bjerrum-Möller & Nielsen (1969*a*,*b*) for the three-axis neutron spectrometer. We may therefore take over directly their expressions for the widths of inelastic scans through phonon dispersion surfaces. It is unlikely that these will be of immediate practical use however!

Double-monochromator case

In many cases, in particular at synchrotron sources, it is convenient to use a monochromator composed of two parallel crystals. Such a double monochromator may be treated by the independent distribution method provided both crystals are of similar material and the same reflecting planes are used in each crystal. An additional restriction is that the first monochromator should be symmetrically cut with $b = -1$. However, even when the latter condition is not satisfied $R(\delta\mathbf{Q})$ can still be written as a one-dimensional integral [*cf.* (27)]. Equations (23) and (26) are retained with α_M and β_M calculated for the *second* monochromator crystal. An additional multiplicative factor appears in (25) and (28) to represent the diffraction characteristics of the first monochromator crystal. In (25) the additional term is $D_M\{[(B_0 + B_2 x_2) + x_2 \sin u_2(1 + b_1)]/X_1|b_1 b_2|^{1/2}\}$, where u_2 and X_1 are defined by (23) and (26) in terms of the parameters of the *second* monochromator. The surface cuts of the first and second monochromator crystals are represented by b_1 and b_2 respectively.

Measurement of the resolution function with a perfect-crystal sample

The resolution profile $R(\delta Q)$ calculated above cannot be measured directly. However, if a sample whose Darwin width is less than those of the monochromator and analyser is available reasonably accurate measurement can be achieved. If the sample is a symmetrically-cut perfect crystal the 'ideal' Bragg δ function assumed in (27) is spread in the direction of τ and is distributed according to the Darwin function of the sample. Thus the measured scattering is given by convoluting $R(\delta Q_\parallel, \delta Q_\perp)$ calculated above with the sample Darwin profile. Specifically

$$J(\delta Q_\parallel, \delta Q_\perp) = \int R(\delta Q_\parallel - x, \delta Q_\perp)\, D_s(y)\, \mathrm{d}x, \quad (31)$$

where

$$y = \frac{2(n-1) + x \sin\theta_B/k}{K|\psi'_H|} \quad (32)$$

and all quantities in (32) refer to the sample crystal.

Measurements of $J(\delta Q_\parallel, \delta Q_\perp)$ were performed with a triple-axis X-ray spectrometer at a 12 kW high-brilliance rotating-anode generator at Brookhaven National Laboratory. The characteristic radiation Mo $K\alpha_1$ (λ = 0·70926 Å, $\Delta\lambda_{\mathrm{FWHM}}$ = 0·00029 Å) or Cu $K\alpha_1$ (λ = 1·54051 Å, $\Delta\lambda$ = 0·00058 Å), emitted from a source of effective height 1·0 mm and of width 0·5 mm, was monochromated by the 111 reflection of a perfect germanium crystal. This crystal, which had a surface area of 25 × 25 mm, was located 220 mm from the source. In order to investigate a wide variety of resolution functions, either Ge(111), Ge(220), Ge(333) or Si(111) was mounted on a sample table which was 450 mm from the monochromator. The analyser was identical with the monochromator [Ge(111)] and it was set in either the parallel or the antiparallel configuration 450 mm away from the sample. The detector was a scintillation counter with about 1 keV energy resolution. The X-ray beam incident upon the sample was made as small as 0·2 × 0·2 mm by a slit. No collimators were placed between optical elements. All perfect crystals used in the present measurements were symmetrically cut ($b = -1$).

The resolution function convoluted with a sample response function [see (31)] in the transverse ($\delta Q_\perp$) or longitudinal ($\delta Q_\parallel$) direction was obtained by rocking the sample (θ_s) or by scanning the sample and analyser arm in a ratio of 1:2 ($\theta_s - 2\theta_s$). Both θ_s and $2\theta_s$ axes had a high angular precision of 0·0005°, sufficient for high-resolution measurements. In the comparisons between observations and calculations presented below, we define a spectrometer configuration by the notation: $M(hkl)^{\varepsilon}$–$S(hkl)^{\varepsilon}$–$A(hkl)^{\varepsilon}$. Here M, S and A denote the type of crystal used for monochromator, sample and analyser respectively, (hkl) is the index of the diffracting planes of the crystal and the superscript, ε, denotes the scattering sense. As for (23) and (24), $\varepsilon = +1$ for scattering to the right and $\varepsilon = -1$ for scattering to the left. Accordingly, the symbol $\mathrm{Ge(111)^+}$–$\mathrm{Ge(333)^-}$–$\mathrm{Ge(111)^+}$, for example, indicates that both monochromator and analyser are Ge(111) while the sample

is Ge(333). Furthermore, these three elements are set in the W configuration.

Comparison with experiments

When three symmetrically cut crystal elements are identical and perfectly parallel, the monochromator and analyser systems bear a special relationship to one another since $u_2 = u_4 = -\theta_B$ [*cf.* (23) and (24)]. In this case, the fact that the monochromator and analyser crystals obey dynamical diffraction theory leads to a distinctive intrinsic resolution function, when the sample scattering is assumed to be a δ function. Fig. 4(*a*) shows one such example calculated for the Ge(111)$^+$–Ge(111)$^-$–Ge(111)$^+$ configuration and Mo $K\alpha_1$ radiation. In this figure, the abscissa and the ordinate represent $\delta Q_{\parallel}$ and $\delta Q_{\perp}$. Both quantities are measured from the maximum of the calculated resolution function, which usually does not coincide with the kinematical Bragg point marked by a star in the figure because X-rays are refracted in a crystal. The resolution function is drawn as a set of eqi-probability contours with R = 100, 75, 50 and 25%.

If we use (31) to convolute the intrinsic resolution with the Darwin function of a sample, the peculiar shape is suppressed as shown in Fig. 4(*b*). The latter figure should be compared with Fig. 4(*c*) which is the resolution function measured by the method described in the preceding section. Measurements were made at each marked point in Fig. 4(*c*) around the $\mathbf{Q} = (1,1,1)$ reciprocal-lattice point and interpolated contours were drawn. Since an absolute scattering angle was not measured, the observed peak position has been placed so as to coincide with the maximum of the calculated resolution function. We obtain very good agreement between calculation and observation. Fig. 5 shows such a comparison of calculation and experiment along the $\delta Q_{\parallel}$ direction with $\delta Q_{\perp} = 0$. The relative momentum resolution in this case is obtained as $\Delta Q_{\mathrm{FWHM}}/Q = 3{\cdot}9 \times 10^{-4}$ and $5{\cdot}2 \times 10^{-5}$ in the longitudinal and transverse direction, respectively.

The symmetric configuration of monochromator and analyser systems with respect to the sample position results in a symmetric resolution function with respect to the $\delta Q_{\parallel}$ axis as seen in Fig. 4. If we break this symmetry in the spectrometer set-up by placing the analyser in the antiparallel configuration, the resolution function tilts from the $\delta Q_{\parallel}$ axis as shown in Fig. 6.

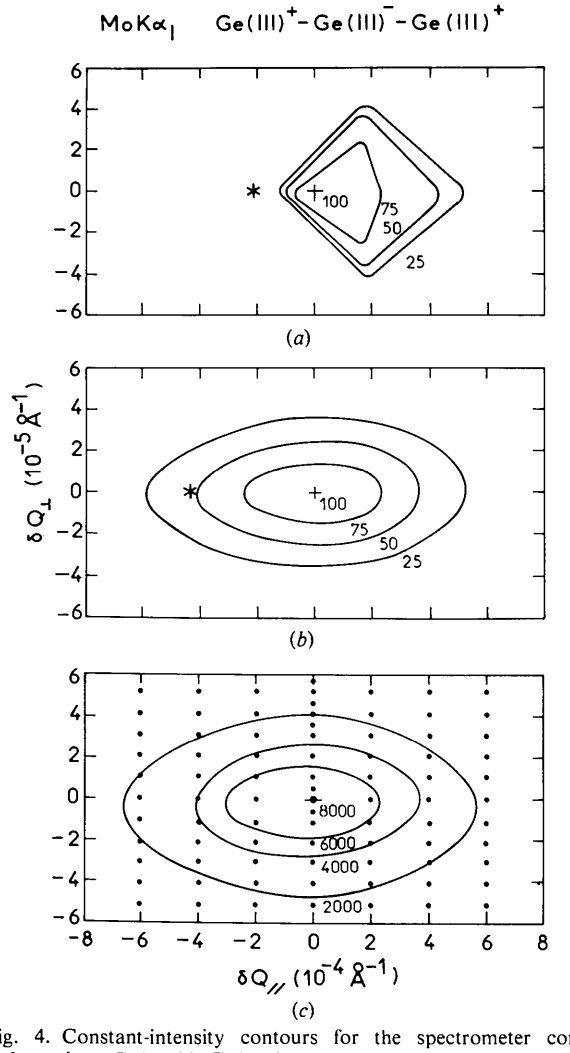

Fig. 4. Constant-intensity contours for the spectrometer configuration Ge(111)$^+$–Ge(111)$^-$–Ge(111)$^+$ as a function of spectrometer misset defined by $\delta Q_{\parallel}$ and $\delta Q_{\perp}$. Mo $K\alpha_1$ radiation is used. (*a*) Contours calculated from (28) assuming that the sample Bragg peak is a Dirac δ function. (*b*) Contours calculated from (31) with the sample scattering properties correctly included. (*c*) Measured contours to be compared with (*b*). The points represent the positions in **q** space at which measurements were made. In (*a*) and (*b*) the star represents the position at which the kinematical Bragg condition is satisfied.

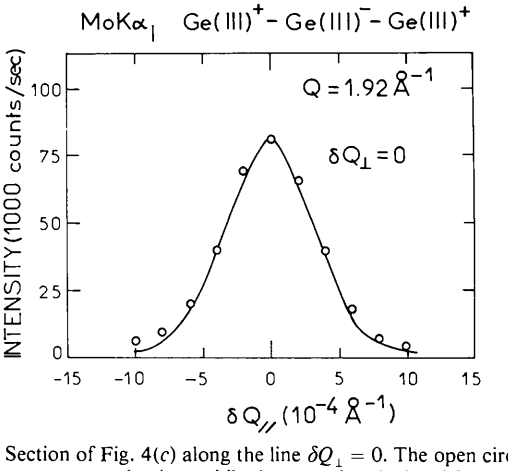

Fig. 5. Section of Fig. 4(*c*) along the line $\delta Q_{\perp} = 0$. The open circles represent measured values while the curve is calculated from (31) and normalized to the peak intensity of the experimental curve.

The calculation (Fig. 6*b*) for Ge(111)$^+$–Ge(111)$^-$–Ge(111)$^-$ agrees well with the observation (Fig. 6*c*) in both the size of the resolution function and its tilt angle.

Fig. 7 represents the case in which Ge(333) is used as a sample while Ge(111) is used for both monochromator and analyser. Although the spectrometer has a symmetric *W* configuration, the peculiar shape of the intrinsic resolution function shown in Fig. 4(*a*) is hardly seen (Fig. 7*a*) because the three crystal elements are no longer parallel. That is, a special relationship among u_i's no longer holds in this case.

A final example is given in Fig. 8, in which the Cu $K\alpha_1$ radiation was used for the Ge(111)$^+$–Ge(220)$^-$–Ge(111)$^+$ configuration. The comparison is made only along the principal axes $\delta Q_\parallel$ and $\delta Q_\perp$. Fig. 8(*a*) shows in fact the maximum disagreement between calculation and measurement which we have been able to find.

Conclusions

In this paper we have developed a formalism which allows the resolution of a three-axis perfect-crystal spectrometer to be calculated for conventional or synchrotron radiation X-ray sources. The method is straightforward to apply and, as far as we have been able to test, gives reliable estimates of resolution properties.

This work was performed while Roger Pynn was a summer guest at Brookhaven National Laboratory and he would like to thank the staff of the BNL Physics Department for their hospitality. The authors would like to thank J. D. Axe, S. Kikuta and T. Matsushita

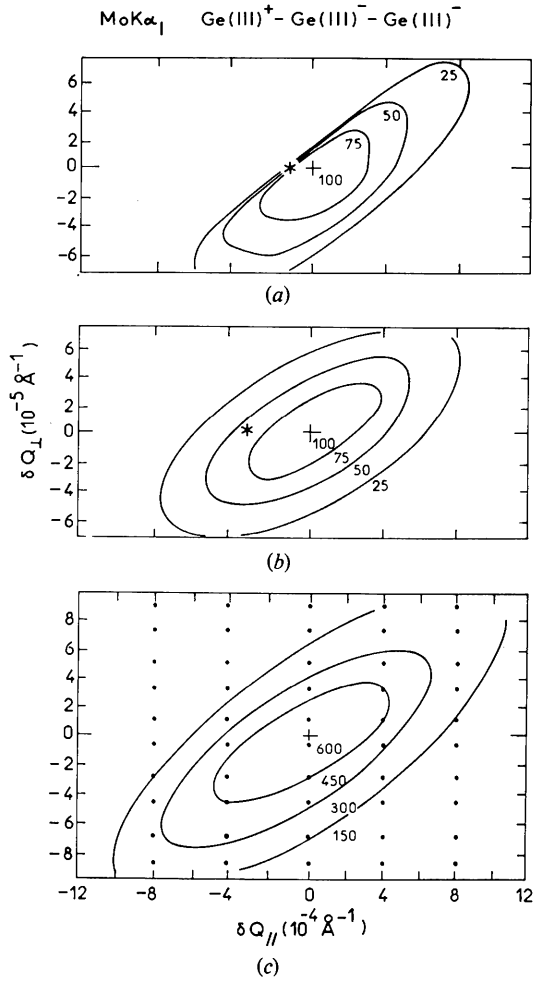

Fig. 6. Constant-intensity contours for the spectrometer configuration Ge(111)$^+$–Ge(111)$^-$–Ge(111)$^-$. For details see the caption of Fig. 4.

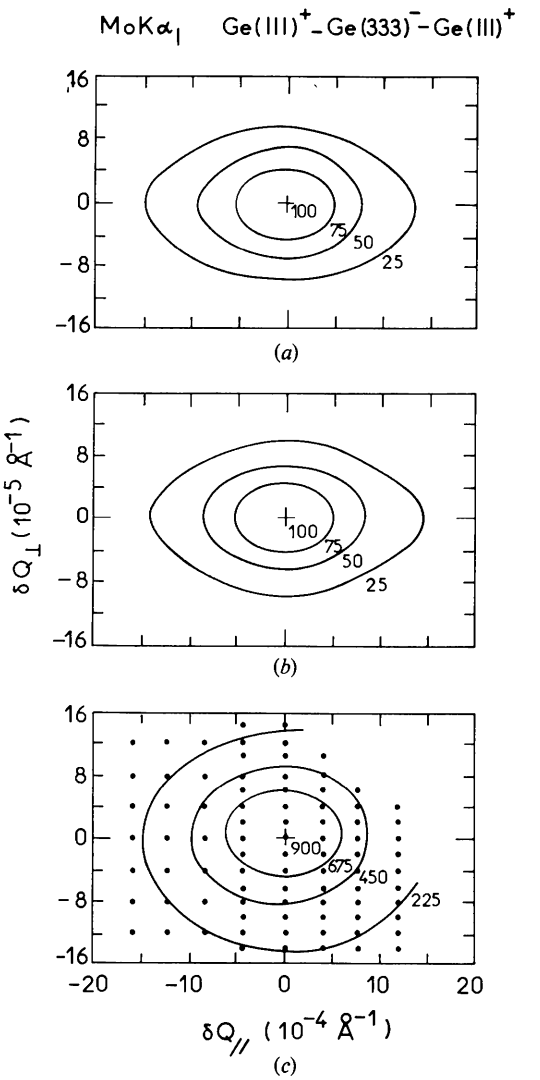

Fig. 7. Constant-intensity contours for the spectrometer configuration Ge(111)$^+$–Ge(333)$^-$–Ge(111)$^+$. See the caption of Fig. 4 for an explanation of the different parts of the figure.

for useful discussions and H. Yoshizawa for help with the measurements of the resolution functions. Work at Brookhaven was supported by the Division of Basic Energy Sciences, US Department of Energy, under contract No. DE-AC02-76CH00016.

APPENDIX

The calculation presented in the body of the paper referred specifically to a conventional source. It is possible to perform the same calculation for a synchrotron radiation source which is assumed to produce white radiation over the range of interest. If the inherent collimation of the synchrotron source is η (standard deviation) we may replace (19) by

$$P_1(\theta_1,k) = \exp -\frac{1}{2}\left(\frac{\Delta_2^{\perp}}{b\eta}\right)^2. \qquad (A1)$$

Then we find that (23) is replaced by

$$u_1 = 0; \quad \tan(\varepsilon_M \varepsilon_s u_2) = \alpha_M/\beta_M \qquad (A2)$$

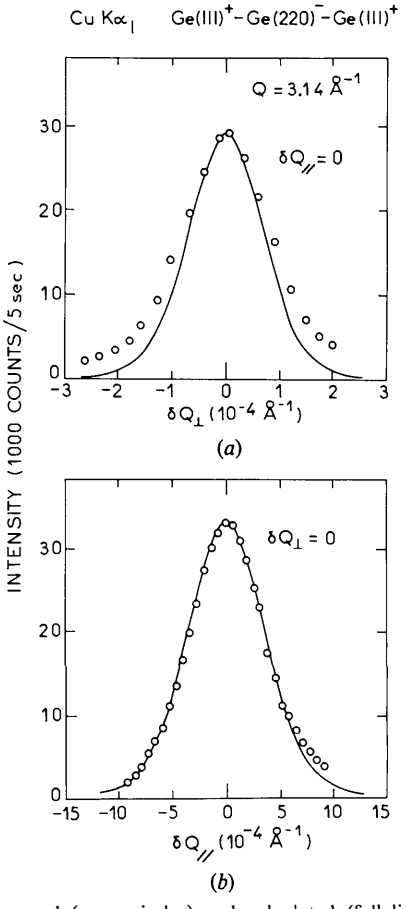

Fig. 8. Observed (open circles) and calculated (full line) profiles obtained with Cu $K\alpha_1$ radiation and a spectrometer configuration Ge(111)$^+$–Ge(220)$^-$–Ge(111)$^+$.

and (26*a*) and (26*b*) by

$$X_1 = k/\alpha_M$$
$$X_2 = kb\eta/\sin u_2. \qquad (A3)$$

The integral of (27) is performed in the same way to give (28) but with the definitions

$$A_0 = -\delta Q_{\perp}/|\tan u_4 \cos\theta_s|$$
$$A_1 = 2\tan\theta_s \cot u_4 + 1$$
$$A_2 = |\cos u_4 \sin(\theta_s + u_2) + \cos u_2 \sin(\theta_s + u_4)|/|\cos\theta_s \sin u_4|$$
$$B_0 = \frac{\delta Q_{\parallel} \sin\theta_s - \delta Q_{\perp} \cos\theta_s}{2\sin^2\theta_s}$$
$$B_2 = -\sin(\theta_s + u_2)/\sin\theta_s \qquad (A4)$$

For a double monochromator (*A*2) and (*A*3) above refer to the second monochromator and an extra multiplicative term $D_M\{|B_0 + B_2x_2 + x_2\cos u_2(1 + b_1)/b_1|b_1|^{1/2}/X_1|b_2|^{1/2}\}$ appears in (28). In this term b_1 and b_2 describe the surface cuts of the first and second monochromator respectively; u_2 and X_1 are defined by (*A*2) and (*A*3) in terms of the parameters of the second monochromator.

Recently, Matsushita & Kaminaga (1980) have developed a method for estimating the performance of various optical systems installed at a synchrotron radiation source. These authors have calculated the shape of the photon distribution function $P_i(k_i)$ [*cf.* (14)] for various cases, including those in which bent crystals and elliptic mirrors are used.

References

ALS-NIELSEN, J., LITSTER, J. D., BIRGENEAU, R. J., KAPLAN, M., SAFINYA, C. R., LINDEGAARD-ANDERSEN, A. & MATHIESEN, S. (1980). *Phys. Rev. B*, **22**, 312–320.

BATTERMAN, B. & COLE, H. (1964). *Rev. Mod. Phys.* **36**, 681–717.

BIRGENEAU, R. J., BROWN, G. S., HORN, P. M., MONCTON, D. E. & STEPHENS, P. W. (1981). *J. Phys. C*, **14**, L49–L54.

BJERRUM-MÖLLER, H. & NIELSEN, M. (1969*a*). *Proceedings of IAEA Panel Meeting on Instrumentation for Neutrons*. Vienna: IAEA.

BJERRUM-MÖLLER, H. & NIELSEN, M. (1969*b*). *Acta Cryst.* A**25**, 547–552.

COOPER, M. J. & NATHANS, R. (1967). *Acta Cryst.* **23**, 357–367.

DARWIN, C. G. (1914). *Philos. Mag.* **27**, 325–331, 675–690.

KIKUTA, S. (1970). *J. Phys. Soc. Jpn*, **30**, 222–227.

KIKUTA, S. & KOHRA, K. (1970). *J. Phys. Soc. Jpn*, **29**, 1322–1328.

MATSUSHITA, T. & KAMINAGA, U. (1980). *J. Appl. Cryst.* **13**, 465–471, 472–478.

NIELSEN, M., ALS-NIELSEN, J., BOHR, J. & MCTAGUE, J. P. (1981). *Phys. Rev. Lett.* **47**, 582–586.

SINHA, S. K. (1980). *Ordering in Two Dimensions*. Amsterdam: North Holland.

STEDMAN, R. (1968). *Rev. Sci. Instrum.* **39**, 878–883.

ZACHARIASEN, W. H. (1945). *Theory of X-ray Diffraction in Crystals*. New York: Wiley.